

Allen Cell Types Database

TECHNICAL WHITE PAPER: CELL MORPHOLOGY AND HISTOLOGY

OVERVIEW

This document describes the overall process for gathering detailed cell morphology information, generated from images acquired from tissue sections *in situ* and from reconstructions of individual neurons. Sectioning processes and immunohistological staining for human neurosurgical tissue are discussed. Methods are described for histological staining of biocytin-filled cells, from either human or mouse specimens labeled during whole-cell patching of somata after electrical stimulation. For the morphological analysis of mouse neurons, fluorescent and brightfield images were acquired at whole-section or single cell resolution. Images (20X magnification) were evaluated to aid in determining the orientation, laminar position and anatomical location of each cell. Serial images (63X magnification) through biocytin-filled neurons were evaluated for quality, and cells that passed a quality threshold entered a detailed morphological analysis workflow. Reconstructions of cell dendrites and the initial segment (spiny neurons) or complete axon (aspiny neurons) were generated for a subset of neurons using a 3D Visualization-Assisted Analysis (Vaa3D) workflow. The automated 3D reconstruction results were then manually curated using the Mozak extension of Vaa3D. Quantitative morphological feature measurements were extracted from each final reconstruction data file. These measurements are then displayed via the www.brain-map.org portal and incorporated into biophysical modeling workflows.

RATIONALE AND DESCRIPTION OF MARKER PANEL

Human surgical tissue blocks were sectioned and subjected to a standard panel of histological stains to provide detailed cytoarchitectural information for each specimen. The selection of markers used for histological profiling is summarized below.

- **Nissl** - cytoarchitecture, to assist with identifying plane of section, cortical layer identification/validation.
- **NeuN** - neuronal nuclei; stains for neurons (post-mitotic); provides additional information about cytoarchitecture, plane of sectioning, cortical layer identification/validation.
- **SMI-32** - Neurofilament H (NF-H), non-phosphorylated; neuronal cell bodies, dendrites; provides additional information about cytoarchitecture, plane of sectioning, cortical layer identification/validation.
- **GFAP** - glial fibrillary acidic protein; intermediate filament protein, astrocytes/progenitor cells, provides additional information about glial reactivity, which can be an indication of pathology.
- **Pvalb** - parvalbumin; marker of fast-spiking interneurons; provides additional information about interneuron density, where low density can be a marker of pathology.
- **Iba-1** - ionized calcium binding adaptor molecule 1; calcium binding protein, microglia/macrophage specific, provides additional information about glial reactivity, which can be a marker of pathology.
- **Ki67** - proliferating cells; stains for mitotic neurons, which can be a marker of pathology.

SAMPLING STRATEGY

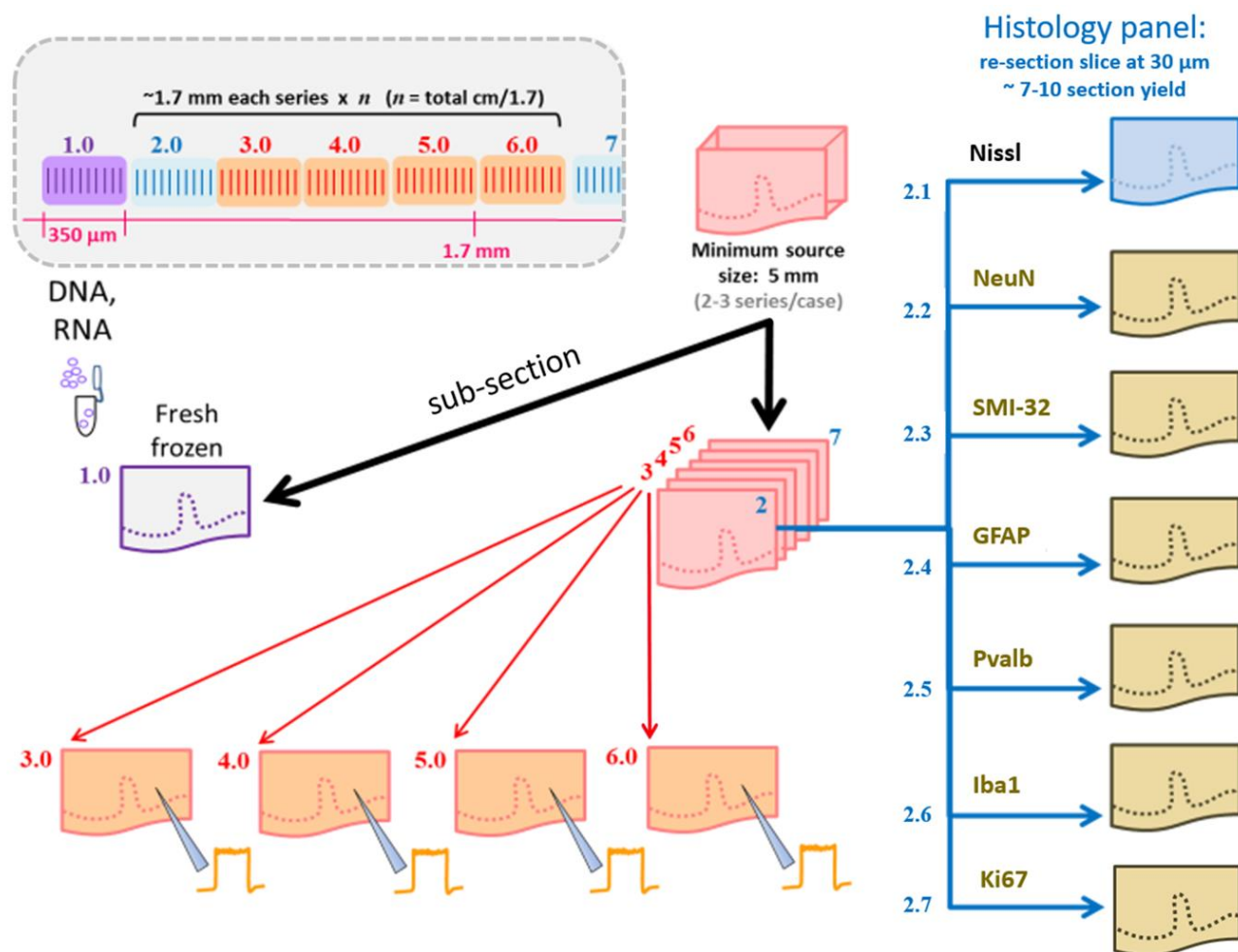


Figure 1. Sampling strategy for for human tissue processing. Thick tissue slices (pink) were prepared for three analysis workflows: transcriptional (frozen for DNA or RNA profiling, in purple), morphoelectric (incubated for patch-clamp recording and biocytin filling cells, in peach), or a histology panel (fixed and re-sectioned; thin sections for Nissl in blue; immunohistochemical markers in beige).

The sampling strategy for human tissue analysis is summarized in **Figure 1**. Briefly, a series of five 350 μm tissue slices was collected every 1.7 mm from surgically excised human tissue blocks (typically 2-3 series collected per case). The first slice in each series was re-sectioned and stained using the seven histochemical markers described. The remaining 4 slices were reserved for patch-clamp recordings and morphological analysis of single cells. One 350 μm slice from every tissue block was fresh frozen and reserved for DNA or RNA analyses.

SLICE PREPARATION FOR HISTOLOGY

Tissue slices (350 μm thick) designated for histological profiling were fixed for 2-4 days in 4% paraformaldehyde (PFA) in phosphate-buffered saline (PBS) at 4°C and transferred to PBS + 0.1% sodium azide for storage at 4°C. Slices were then cryoprotected in 30% sucrose, frozen and re-sectioned at 30 μm using a sliding microtome (Leica SM2000R). Sections were stored in PBS+azide at 4°C in preparation for immunohistochemical and Nissl staining.

IMMUNOHISTOCHEMICAL CHARACTERIZATION OF HUMAN TISSUE

Two different staining protocols were used as outlined below. The protocol was altered to increase slide staining throughput, specificity of signal to noise ratio, and establish a fully automated immunohistochemical staining platform on the Biocare IntelliPATH FLX® Slide Stainer.

IHC Protocol Version 1: This protocol was used exclusively for all immunohistochemical (IHC) staining through August 8, 2017.

NeuN, Parvalbumin, SMI-32, GFAP, and Iba-1

Free floating sections (30 µm) were stained in 24-well plate inserts. Sections were washed in PBS-Tween 20 (0.05%) and endogenous peroxidase activity was blocked using 3% hydrogen peroxide in PBS. Sections were washed in PBS-Tween 20 before incubation in blocking solution containing 4% horse serum (Vector Laboratories) and 0.3% Triton-X in PBS. Sections were then incubated with primary antibodies (see **Table 1** for antibody information) diluted in blocking solution overnight. The following day, sections were rinsed in PBS-Tween 20 before incubation in a biotinylated secondary antibody (Vector Laboratories) prepared in blocking solution. Sections were rinsed in PBS-Tween, incubated for 30 min in ABC (Vectastain, Vector Laboratories), and the reaction product visualized with 0.05% DAB (Sigma-Aldrich), containing 0.003% hydrogen peroxide. Sections were washed a final time in PBS, dehydrated through graded alcohols, cleared with Formula 83, and coverslipped with DPX. Slides were subjected to quality control (QC) assessment and stored at room temperature prior to digital imaging.

Ki67

Sections (30 µm) were mounted on gelatin-coated slides and allowed to dry before being hydrated in PBS and incubated in 10mM sodium citrate at 98°C. Slides were allowed to cool, then washed in PBS-Tween 20 (0.05%) and endogenous peroxidase activity was blocked using 3% hydrogen peroxide in PBS. Slides were washed in PBS-Tween 20 before incubation in blocking solution containing 4% horse serum (Vector Laboratories) and 0.3% Triton-X in PBS. Slides were then incubated with primary antibody diluted in blocking solution overnight (see **Table 1** for antibody information). The following day, slides were rinsed in PBS-Tween 20 before incubation in biotinylated secondary antibody (Vector Laboratories) prepared in blocking solution. Slides were rinsed in PBS-Tween, incubated for 30 min in ABC (Vectastain, Vector Laboratories), and the reaction product visualized with 0.05% DAB (Sigma-Aldrich), containing 0.003% hydrogen peroxide. Slides were washed a final time in PBS, counterstained with hematoxylin, dehydrated through graded alcohols, cleared with Formula 83, and coverslipped with DPX. Slides were subjected to QC assessment and stored at room temperature prior to digital imaging.

Table 1. Immunohistochemistry staining protocol conditions

	Neu-N	SMI-32	GFAP	Parvalbumin	Iba-1	Ki67
Antibody Vendor	Millipore #MAB377	Biologend #801704	Millipore #MAB360	Swant #PV 235	Wako #019-19741	Dako #M724001-2
Staining Method	Floating	Floating	Floating	Floating	Floating	Mounted on slide
Pre-treatment	N/A	N/A	N/A	N/A	N/A	Sodium Citrate AR
Primary antibody dilution	1:1000	1:1000	1:1000	1:1000	1:2000	1:200
Secondary antibody dilution	Anti-mouse 1:200	Anti-mouse 1:200	Anti-mouse 1:200	Anti-mouse 1:200	Anti-rabbit 1:200	Anti-mouse 1:200
Post-stain process	Mount, Dehydrate, DPX	Counterstain, Dehydrate, DPX				

IHC Protocol Version 2: This protocol was used exclusively for all immunohistochemical (IHC) staining after August 9, 2017.

For IHC staining: NeuN, Parvalbumin, SMI-32, GFAP, IBA-1 and Ki67 detection

Prepare and mount slides the day prior to IHC staining

Free floating sections (30 µm) were pre-mounted onto gelatin coated slides, the day prior to IHC staining and first allowed to dry flat at room temperature for 30-60 minutes, then were briefly rinsed in Milli-Q water. All slides were placed in a 37°C oven overnight prior to IHC staining the following day.

Day of IHC staining: Neu-N, Parvalbumin, SMI-32, GFAP, Iba-1 and Ki67 detection

Peroxidase Blocking Preparation: All slides were washed in Biocare 1X TBS wash buffer (Biocare#: TWB945M) and endogenous peroxidase activity was blocked using 3% hydrogen peroxide in 1X TBS wash buffer.

Heat Induced Epitope Retrieval (HIER): All slides underwent Heat Induced Epitope Retrieval (HIER) in a 98°C Sodium Citrate buffer bath, pH 6.0 for 20 minutes, then allowed to cool at room temperature for 20 minutes. All slides were rinsed in Milli-Q water and equilibrated using 1X TBS buffer. All antibodies were diluted in Renaissance Background Reducing Diluent (Biocare #PD905L). All slides were loaded onto the Biocare IntelliPATH FLX® Automated Slide Stainer and stained with the following conditions: Slides were incubated in Background Punisher (Biocare #BP974M) then immediately incubated in primary antibodies (see **Table 2** for antibody dilutions and stain conditions).

Table 2. Summary of antibody dilutions and conditions.

	Neu-N	SMI-32	GFAP	Parvalbumin	Iba-1	Ki67
Antibody Vendor	Millipore #MAB377	Biologend #801704	Millipore #MAB360	Swant #PV235	Wako #019-19741	Dako #M724001-2
Staining Method	intelliPATH FLX®	intelliPATH FLX®	intelliPATH FLX®	intelliPATH FLX®	intelliPATH FLX®	intelliPATH FLX®
Pretreatment	Sodium Citrate, 20'	Sodium Citrate, 20'	Sodium Citrate, 20'	Sodium Citrate, 20'	Sodium Citrate, 20'	Sodium Citrate, 20'
Primary Ab °	1:2000	1:2000	1:1500	1:2000	1:1000	1:200
Secondary reagent (Biocare)	Biocare Ms Secondary Reagent (10')	N/A	Biocare Ms Secondary Reagent (10')			
Tertiary reagent (Biocare)	Universal HRP Tertiary (15')	Universal HRP Tertiary (30')	Universal HRP Tertiary (15')			
Hematoxylin Counterstain (Biocare)	N/A	N/A	N/A	N/A	N/A	20/80 Mix
Post-Staining	Mount, Dehydrate, DPX	Mount, Dehydrate, DPX	Mount, Dehydrate, DPX	Mount, Dehydrate, DPX	Mount, Dehydrate, DPX	Mount, Dehydrate, DPX

All slides were programmed using the IntelliPATH FLX® protocol run plan (See **Table 3** and **Table 4**) and rinsed on an autostainer using 1X TBS wash buffer (Biocare #TWB945M). All slides, with the exclusion of (rabbit) IBA-1 were incubated in Mouse Secondary Reagent (Biocare#: IPSC5001G20), rinsed with 1X TBS and incubated in Universal HRP Tertiary Reagent (Biocare #: IPT5002G20), with or without the decant (blow) step. All slides were rinsed in 1X TBS and incubated in IP FLXDAB (Biocare Buffer #IPBF5009G20 and DAB Chromogen (Biocare Chromogen# IPC5008G3), rinsed in 1X TBS and incubated in DAB Sparkle (Biocare#: DSB830M).

With the exception of Ki67, all slides are rinsed in 1X TBS wash buffer and rinsed in Milli-Q water. Ki67 slides were rinsed in Milli-Q water following the DAB Sparkle incubation step and counterstained in Hematoxylin (Biocare#: IPCS5006G20), using a 20/80 ratio of Hematoxylin to Milli-Q water. All slides were rinsed in 1X TBS, followed by a final rinse in Milli-Q water. Upon autostainer run completion, all slides were unloaded into Milli-Q water, dehydrated through a series of graded alcohols, cleared with Formula 83, and coverslipped with DPX. Slides were subjected to QC assessment and stored at room temperature prior to digital imaging.

Table 3. IntelliPATH FLX® staining protocol, excluding Ki67.

Step #	Process	Blow	Reagent	Volume (µl)	Time (min)	Wash	Count
1	Pre-Treatment	X	Citrate	200	00:20	Buffer 1	1
2	Block	√	Background Punisher	200	00:10	Buffer 1	1
3	Antibody	X	Antibody, diluted	200	01:15	Buffer 1	2
4	Secondary	X	Mouse Secondary Reagent	200	00:10 [Iba-1-N/A]	Buffer 1	2
5	Tertiary	X	Universal HRP Tertiary	200	00:15 [Iba-1-30']	Buffer 1	2
6	Chromogen	X	IP FLX DAB	200	00:05	Buffer 1	1
7	Chromogen	X	Biocare Sparkle	300	00:01	mQH ₂ O	2
9	Wash				00:00	Buffer 1	1
10	Wash				00:00	mQH ₂ O	2

Table 4. IntelliPATH FLX® staining protocol for Ki67.

Step #	Process	Blow	Reagent	Volume (µl)	Time (min)	Wash	Count
1	Pre-Treatment	X	Citrate	200	00:20	Buffer 1	1
2	Block	√	Background Punisher	200	00:10	Buffer 1	1
3	Antibody	X	Ki67 (1:200)	200	01:15	Buffer 1	2
4	Secondary	X	Mouse Secondary Reagent	200	0:10	Buffer 1	2
5	Tertiary	X	Universal HRP Tertiary	200	0:15	Buffer 1	2
6	Chromogen	X	IP FLX DAB	200	00:05	Buffer 1	1
7	Chromogen	X	Biocare Sparkle	300	00:01	mQH ₂ O	2
8	Counterstain	X	20/80 Hemaxtoylin	200	00:01	mQH ₂ O	1
9	Wash				00:00	Buffer 1	1
10	Wash				00:00	mQH ₂ O	2

Nissl Staining

Sections (30 µm thick) mounted on gelatin-coated slides were stored at 37°C for 1–7 days and were removed 5–15 minutes prior to staining. Sections were defatted with the xylene substitute Formula 83 (CBG Biotech), and hydrated through a graded series containing 100%, 95%, 70%, and 50% ethanol. After incubation in water, the sections were stained in 0.213% thionin, rinsed in water and dehydrated in a graded series containing 50%, 70%, and 95% ethanol before being differentiated in 95% ethanol containing 0.1% glacial acetic acid. Once sufficiently differentiated, sections completed dehydration series in 95% and 100% ethanol. Finally, the slides were incubated in Formula 83, and coverslipped with the mounting agent DPX (VWR #100503-834). After drying, the slides were analyzed microscopically to ensure staining quality. Slides that passed QC were stored at room temperature in slide boxes before being cleaned in preparation for imaging.

Slide Imaging

Colorimetric IHC and other histologically-stained whole slides (*i.e.* Nissl-stained preparations) for brightfield imaging were scanned using an Aperio ScanScope XT slide scanner (Leica Biosystems, Germany). An AutoLoader rack allowed up to 120 1x3" slides to be loaded in a single batch. The scanning method employed a linear array detector using full dynamic range determination and automatic tissue- and focus-finding features. The focus point map and scan area settings were inspected and adjusted by operators prior to each scan, and the line camera continually adjusted for focus to correct for variation in the tissue focal plane. The samples were illuminated using a 21DC Halogen Lamp (Techniquip, USA). Brightfield images were acquired using ScanScope Console (v101.0.0.18) and controller (ve101.0.4.446) at 10x magnification (objective lens 20x/0.75 NA Plan Apo, 0.5x magnifier) resulting in a pixel size of 1.0 $\mu\text{m}/\text{pixel}$. Acquired images were exported in SVS file format using Spectrum (v10.2.2.2317) and managed via a custom Laboratory Information Management System (LIMS). During image QC review, a bounding box was manually adjusted to capture individual tissue sections. The image QC check included qualitative inspection for focus, line stitch alignment, even illumination and image cutoff. Images additionally failed the QC check if data analysis was compromised by artifacts, such as section damage or mounting media bubbles.

Image Analysis

IHC staining was performed on tissue from each human neocortical surgical specimen in order to evaluate the integrity of the sample. In all cases, the excised tissue was distal to the pathological focus or tumor and deemed to be relatively neurotypical with regards to cytoarchitecture and laminar organization. Clinical or pathological analyses are not performed, and would be needed to fully assess potential cellular and circuit level alterations related to patient disease state.

IMMUNOHISTOLOGY

DAB Detection of Biocytin Filled Cells

Protocol Version 2: Version 2 has been used since May 17, 2016 for all IHC staining.

An HRP enzyme reaction using DAB as chromogen was used to visualize the filled cells after electrophysiological recording. Tissue slices containing biocytin filled cells were fixed in 4% PFA/2.5% glutaraldehyde for 40-48 hours at 4°C on an orbital shaker (note previous protocol omitted glutaraldehyde, as summarized in **Table 5**). For weekend and extended weekend fixation, slices were maintained in 4% PFA/2.5% glutaraldehyde for 71 to 95 hrs. Slices were then transferred to 1X PBS at 4°C for 1-10 days prior to staining. Slices were placed in 5 μM DAPI in PBS for 15 min then rinsed with 1X PBS(+) (1X PBS with 0.0005% Tween-20) three times, incubated in 1% H_2O_2 for 30 min to block endogenous peroxidases, and rinsed in 1X PBS(+) another three times. The tissue was then permeabilized by incubation in ABC (Vectastain, Vector Laboratories) in PBS with 5% Triton for 60 min at room temperature and then incubated for 2 days (>40 hours) at 4°C.

Table 5. Staining protocols for DAB detection of biocytin filled cells.

Step	Stage	Version 1 Staining prior to May 17, 2016	Version 2 Staining after May 17, 2016
Fixative	Fixation	4% PFA	4% PFA/2.5% Glutaraldehyde
Fix duration	Fixation	Overnight	40 - 48 hours
ABC detergent	Histology	60 minutes of 2% Triton, Followed by ABC with 0.1% Triton overnight	5% Triton included with overnight ABC
ABC incubation length	Histology	Overnight	> 2 days
Nickel-enhanced DAB	Histology	Yes	No
Osmium post-fix	Histology	Yes	No

After the extended overnight incubation (>40 hours), slices were incubated for another 60 min at room temperature in the ABC reagent. Tissue was then washed with 1X PBS(+) three times prior to visualization of the peroxidase product with a 0.05% DAB and 0.3% H_2O_2 solution. The DAB incubation time was standardized

to 3 min. After a final series of three washes in 1X PBS, tissue slices were mounted on gelatin-coated slides and coverslipped with glycerol-based Mowiol mounting media. Slides were dried for approximately 2 days prior to imaging. Mowiol mounting media was made in batches of 100ml and contained: 24g glycerol, 9.6g Mowiol 4-88 (Calbiochem 475904), 24ml MilliQ water, and 48ml 0.2M Tris base (pH 8.5). Slides were allowed to dry prior to imaging.

CELLULAR RESOLUTION IMAGE ACQUISITION

Mounted sections were imaged on an upright brightfield and fluorescence AxioImager Z2 microscope (Zeiss, Germany) equipped with an Axiocam 506 monochrome camera (6 megapixels with a 4.54 μm per pixel size) and 0.63X magnifying camera mount adapter. Two-dimensional (2D) images were captured with a 20X objective lens (Zeiss Plan-NEOFLUAR 20X/0.5, 12.6x total magnification yielding 0.360 micron x 0.360 micron effective pixel size) using the Tile & Position and Multi-channel Acquisition modules in the Zeiss Efficient navigation (ZEN) 2012 SP2 software package (Zeiss). Fluorescence excitation was provided by a Lumen Dynamics X-Cite 120 LED or Excelitas X-Cite 120 LED Boost relayed to the sample plane through an excitation filter and dichroic mirror (Zeiss G 365 and FT 395) prior to the objective; emission was collected through the same objective, passing through the dichroic and emission filter (Zeiss BP 445/50; filters and dichroic provided as FT 49 cube) before reaching the camera. For brightfield imaging light provided by the TI VIS-LED lamp was emitted from the condenser before passing through the sample, objective, and onto the camera with no filter cube in the optical path. Image QC included a qualitative evaluation of signal-to-noise for the imaged object (with high signal apparent in the cell body and dendrites, as opposed to background stain in the surrounding tissue, which can occur when cell filling leaks), utilization of the full available imaging dynamic range, in-focus cell body, high contrast, and absent or negligible tessellation (*i.e.* tiling and stitching edge artifacts). Overall evenness of section illumination and bounding box region for target tissue inclusion was evaluated.

Individual cells were imaged at higher resolution for the purpose of automated and manual reconstruction. Series of 2D images of single neurons were captured with a 63X objective lens (Zeiss Plan APOCHROMAT 63X/1.4 oil, 39.69x total magnification, and an n oil-immersion condenser 1.4 NA), using the Tile & Position and Z-stack ZEN 2012 SP2 software modules (Zeiss). The composite 2D tiled images with X-Y effective pixel size of 0.114 micron x 0.114 micron were acquired at an interval of 0.28 μm along the Z-axis.

Full dynamic range was achieved with a minimum 20 ms exposure time and an optimal TI VIS-LED lamp voltage control adjustment. Individual image tiles were stitched to achieve a full section field of view with a minimum of 5% overlap and a 10% maximum shift. Image QC included a z-stack plane count, a visual check for successful stitching alignment and even illumination throughout the full-field images. 63X Z-stacks were evaluated based on quality metrics that could impact cell reconstruction, as opposed to aesthetic quality, such as image contrast, tile stitch fidelity and anomalies that could contribute to discontinuity in neuron image reconstruction. Image “flipping” per section (cell volume and depth not exceeding the objective working distance) and missing or out-of-order image plane sequence were also evaluated. Images were exported from ZEN as 8-bit Big TIFF files. Image series from individual slices or cells are tracked and managed in LIMS.

IDENTIFICATION OF CELL SOURCE: ANATOMICAL REGION AND CORTICAL LAYER

To characterize the position of cells analyzed from mouse brain, a 4-step process was used. Briefly, 20x brightfield and/or fluorescent images of DAPI (4',6-diamidino-2-phenylindole) were analyzed to determine layer position and to some extent, region, of biocytin-filled cells. Soma position was annotated and used to calculate soma depth relative to pia and white matter. Individual cells were then manually placed in the appropriate cortical region and layer within the Allen Mouse Common Coordinate Framework (CCF) (see **Figure 2**) by matching the 20x image of the slice with a “virtual” slice at an appropriate location and orientation within the CCF.

To determine the position within the cortical depth for human cells, DAPI-stained sections were evaluated to provide cytological context for estimating the laminar position of biocytin-filled cells. Soma position was annotated and used to calculate soma depth relative to pia and white matter. Individual cells were manually assigned to a corresponding anatomical area, or “pinned” to a region in MNI space (MNI-ICBM152-T1 template)

based on this evaluation and tissue block placement (see the **Case Qualification and Donor Profiles** in the [Documentation](#) section).

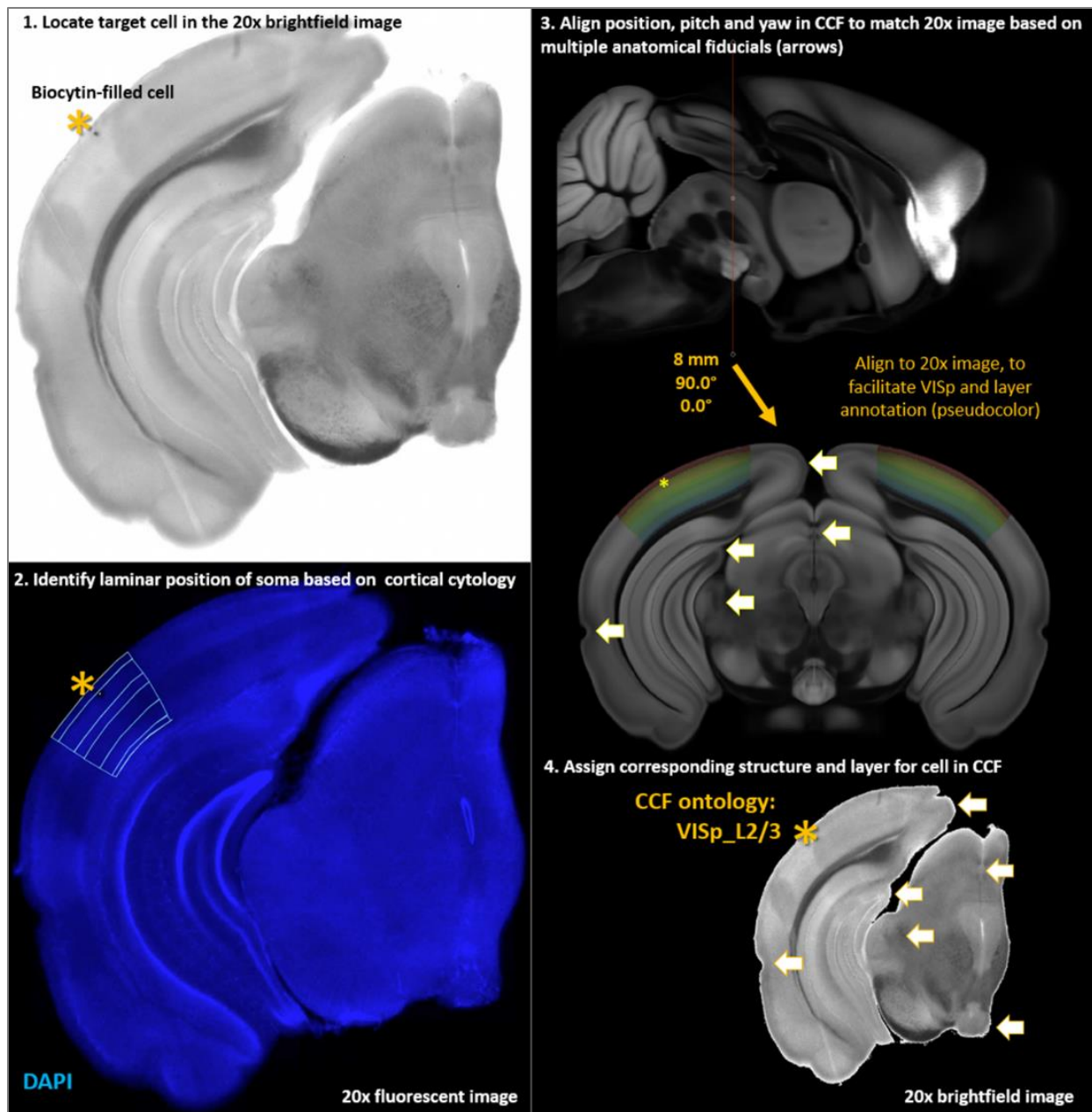


Figure 2. A 4-step anatomical region and layer assignment was performed by manual alignment into the CCF.

MORPHOLOGICAL EVALUATION OF NEURONS

Dendrite Type Assignment

The dendritic morphology of each neuron was identified as either aspiny, sparsely spiny or spiny (Braitenberg and Schuz, 1998 with some modification) based on a qualitative assessment of the neuron’s dendrites by viewing the slides under the microscope, in the 20X or 63X image. These different dendritic types roughly equate to interneurons (aspiny and sparsely spiny) and pyramidal or spiny stellate neurons (spiny). It should be

noted that individual spines were not reconstructed or quantified in these neurons (methods for quantifying spine density to provide a more quantitative basis for classification into these different categories are being investigated).

Aspiny dendrites were defined by the absence of spiny protrusions, lack of a pronounced apical dendrite and/or axon that emerged from the soma or dendrite at odd angles, and had extensive local branching.

Sparsely spiny dendrites were defined by the presence of infrequent to moderately frequent spiny protrusions (approximately one spine per 10 microns), lack of a pronounced apical dendrite and/or an axon that emerged from the soma or dendrite at odd angles, and had extensive local branching, and/or projected up to layer 1. Sparsely spiny neurons were only identified when a 63X image was present.

Spiny dendrites were defined by the presence of frequent spiny protrusions (approximately one spine per 1-2 microns), an axon that descended perpendicularly down to the white matter with sparse, proximal branching occurring at right angles to the primary axonal branch and/or a pronounced primary, apical dendrite.

Apical Intactness

In addition to assigning dendrite type, apical dendrite intactness was categorized for each neuron and defined as the following:

- **Apical dendrite:** A prominent, spiny dendrite that is clearly longer and frequently thicker at its base than all other dendrites. Apical dendrites typically extend toward the pial surface and may or may not end in a tuft.
- **Intact apical dendrite:** An apical dendrite was deemed to be “intact” if the entire length of the *primary* dendritic branch was contained within the thickness of the slice, and was not cut off at either slice surface.
- **Truncated apical dendrite:** An apical dendrite was deemed to be “truncated” if the primary dendritic branch was cut off at either slice surface.

In cases in which a biocytin labeled soma could not be located, or there were not enough dendrites labeled in the slice, the cell was omitted from further analysis.

Annotation of 63X Images

Following an assessment of the quality of the 63X image, the soma was manually delineated on a single representative section, providing both a starting point for automated reconstruction and an estimate of soma radius. Each experimental cell was then assessed to determine if a biologically accurate morphological reconstruction could be achieved. Six major categories were evaluated to determine whether a cell would be reconstructed: tissue quality, neurite integrity, neurite fill, extent of non-specific labeling, drying effects and apical dendrite intactness (when applicable).

All QC categories were considered for each cell, and cells with passing criteria in all categories were prioritized for morphological reconstruction. Tissue quality was determined to be sufficient if tissue damage did not substantially disrupt the integrity of the dendrites. Dendritic integrity was determined to be sufficient if the majority of its dendrites could be identified as either spiny, sparsely spiny or aspiny and were not abnormally beaded or broken. Cell fill was determined to be sufficient if the majority of dendrites were well labeled, including in the Z dimension. For non-specific labeling, a cell passed if the soma or dendrites were not obscured by pipette leakage forming a dark “cloud” around the cell, or causing neighboring cells to be stained, obscuring the primary labeled cell. For tissue drying, a cell passed if the majority of dendrites lacked pronounced tissue drying effects, which can cause the dendrites to appear abnormally kinked or broken. A cell passed for apical dendrite intactness if the apical dendrite of spiny neurons was contained within the slice all along the length of the primary dendrite. Neurons that met each of these criteria were selected for morphological reconstruction. In some cases, neurons that did not meet these criteria were also reconstructed if the morphology and/or electrophysiology were considered to be sufficiently unique or valuable for understanding cortical cell types.

IMAGE PROCESSING AND 3D CELL RECONSTRUCTION OVERVIEW

Microscopy images of single, biocytin-filled neurons passing morphology were subjected to multi-scale enhancement and automated 3D reconstruction to produce a starting point reconstruction that was then extensively, manually curated and corrected to yield a finalized morphological reconstruction of each neuron. The primary steps are as follows:

1. For an individual cell, stitched, multi-tile, 2D image sequences were color inverted and converted to a single 3D image stack.
2. An enhanced 2D image was generated by multi-scale image enhancement on the 2D MIP projection plane from 3D image stack. The output reconstruction (an SWC file) was produced by TReMAP automatic neuron reconstruction.
3. The TReMAP autotrace algorithm was used to process the MIP, and a 2D reconstruction was created. Vaa3D's Virtual Finger was used to map each 2D segment back into the appropriate 3D coordinates in the 3D image stack space.
4. Automatic radius estimation was performed for each node in the reconstruction, and the soma's radius value was applied based on a manual drawing of the outer edge of the soma. The automated reconstruction was manually corrected and curated. This process included deleting false positive branches and connections, adding and extending branches (as dendrite or axon), and then connecting the final structure to yield a complete representation of the dendritic and/or axonal tree within the slice. The radius for each segment was manually applied by interpolation of estimated radii of all branch points and tips.

IMAGE PROCESSING AND 3D CELL RECONSTRUCTION DETAILS

Multi-scale Enhancement

After a cell was selected for reconstruction, the image stack was processed through the informatics pipeline to maximize the signal-to-noise ratio and improve the automatic reconstruction performance, through a customized enhancement (Zhou *et al.*, 2014). The output of the multi-scale enhancement was an enhanced 2D image plane.

SEMI-AUTOMATIC 3D NEURON RECONSTRUCTION

After multi-scale enhancement, an image was then ready for automatic 3D reconstruction. Automatic 3D neuron reconstruction for very large 3D images remains a challenge in neuroscience. For these datasets, an automatic 3D neuron tracing method called TReMAP was developed (Zhou *et al.*, 2016). The key advancement of TReMAP was to utilize 3D Virtual Finger (a reverse-mapping technique) to detect 3D neuron structures based on tracing results on 2D projection planes. TReMAP was used for all data generated after 07/21/2016, while NeuronCrawler was used prior to that date (Zhou *et al.*, 2015).

Tracing the 2D Enhanced Plane

For each labeled group in the 2D enhanced image, 2D projection trees were traced. TReMAP uses All-Path-Pruning 2 (APP2) as the basic tracing module, as APP2 has been shown to be relatively fast and accurate based on pruning a dense initial reconstruction of a neuron to generate a compact representation of the neuron (Peng *et al.*, 2011; Xiao and Peng, 2013).

TReMAP

To prepare for the reverse mapping, the 2D traced neuron tree was broken into a collection of 2D segments first. For each segment, a 2D bounding box was identified and used to extract the corresponding 3D image content for reverse mapping. This divide-and-conquer strategy cuts down the memory consumption of reverse mapping and enables parallel processing to reduce computation time.

A neuron reconstruction can be viewed as a connected graph of many "segments," each being a 3D curve consisting of a number of reconstruction nodes. In the case of a TReMAP reconstruction, each segment corresponds to a 3D curve produced using the Virtual Finger methods. In the end, minimum spanning tree (MST)

was used to connect all 3D curves to produce the final neuron reconstruction. The output file of this process is a single SWC file that ranges from roughly 45KB (~1,000 nodes/compartments) to 450KB (~10,000 nodes/compartments).

CORRECTION AND CURATION OF NEURON RECONSTRUCTION

The automated reconstruction was manually corrected and curated to provide an accurate representation of the dendrites and initial axon (spiny neurons in mouse) or the full neuron (dendrites and axon) within the slice (aspiny and sparsely spiny neurons in mouse; all were reconstructed for human neurons).

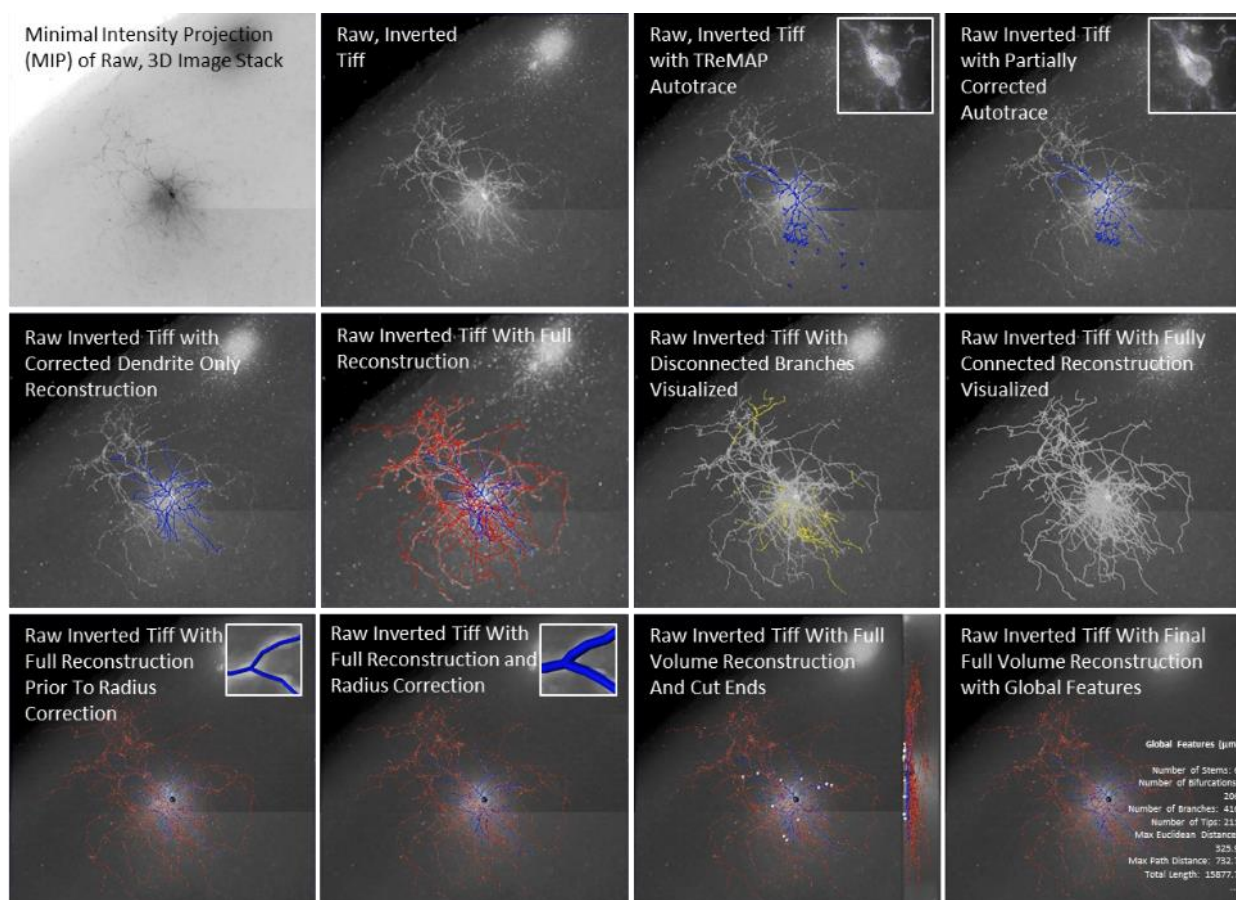


Figure 3. Overview of manual correction and curation of the automated 3D reconstruction using Vaa3D.

Manual reconstruction was performed using the Mozak extension (Zoran Popovic, Center for Game Science, University of Washington) of TeraFly tools (Bria *et al.*, 2016; Peng, Tang *et al.*, 2014) in Vaa3D (3D Visualization-Assisted Analysis) (www.vaa3d.org) (Peng *et al.*, 2010; Peng, Bria *et al.*, 2014). The process begins with inverting the raw images (see **Figure 3**). Reconstructions began with a TReMAP or NeuroCrawler autotrace. First, false positive branches and connections were removed using the “break and/or delete multiple branches by stroke” tool and that soma representation was corrected. The Virtual Finger functions (Peng, Tang *et al.*, 2014) integrated into the Vaa3D platform software were then used for adding and extending dendritic and thicker axonal branches (at the maximum image resolution). For some axons, which can appear as a series of regularly spaced, unconnected puncta, it is necessary to identify the specific z-planes through which the process travels and place nodes at areas of strongest observed signal using the “poly-line” tool. The same image volume in Fiji is sometimes referenced as a high-resolution single plane visual aid.

Every attempt was made to generate a completely connected neuronal structure while still remaining faithful to image data. If axonal processes could not be traced back to the main structure of the neuron, they were left

unconnected. Connected and disconnected axon components (axon cloud) were used to provide perspective on the local axon distribution within the cortex. As a final step in the manual correction and curation process, a QC step by an alternate analyst checked for missed branches or inappropriate connections. Once the reconstruction was complete, multiple plugins were used to standardize node spacing (“Resample_swc”: length = 10 pixels) and node placement around the soma (“inter_node_pruning”), eliminate short, unwanted segments (“Pruning_SWC”: length = 5 nodes), eliminate a jitter artifact caused by reconstruction in a compressed z-dimension (“Z-smooth_SWC”: step size = 10), and order the nodes sequentially within the SWC text file (“IVSCC_sort”).

Manual radius estimation was performed using the “Neuron_radius_interpolation” plug-in, which creates a file containing markers on each dendritic branch node and tip within the reconstruction. The “Assemble_neuron_live” plug-in was then used, which allows the thickness of dendrites at each branch point and tip to be estimated. Finally, the “Neuron_radius_interpolation” plug-in was used to interpolate the estimated radius values to all the nodes in between. An “SWC_slope analysis” plug-in was used to verify that, on average, the dendrites were estimated to be thicker near the soma and thinner near the tips. For further information on requirements for radius representation see the **Biophysical Modeling-All Active** section in the [Documentation](#) tab.

For each reconstruction, quantitative values for morphological features were generated using the “Global_neuron_feature” plug-in (features described below). Dendritic processes that were cut off during slicing or imaging were also indicated as a cut or truncated end by placing an identifying marker at the branch’s terminal node. Axons were treated differently. Only if the axon was cut off very near the soma, was its cut end marked. If the axon continued beyond the proximal soma region, but was not reconstructed, it was marked as “continuing” to indicate that there was more to the axon than was represented in the reconstruction. Dendritic processes that ended naturally within the slice of tissue were left unmarked. The surface of the tissue closest to the soma was also marked. Cut and continuing ends were marked to provide perspective on the completeness of the morphology. In the future, cut end markers may also be used to algorithmically regrow dendritic processes. Soma markers may be used to track tissue shrinkage pre- and post-histology.

Once the SWC and marker file for a neuron were complete, they were processed by a script to automatically check for a variety of common errors. The script identified: disconnected dendrite segments; unusually small soma radii; unusually small or large dendritic radii; branches with an unrealistic taper in their radius estimation; incorrectly spaced nodes; typing mistakes (e.g. an axon node as the parent of a dendritic node); multiple rows in the SWC representing the soma; node types other than soma, basal dendrite, apical dendrite or axon; non-sequential naming of nodes within the SWC; and cut ends markers that were not correctly identified, or did not correspond to the tip of a dendritic branch. If any of these issues were identified for an SWC or marker file, they were manually corrected before the reconstruction was considered complete (implemented in June 2017).

Morphology Features

Reconstructions were saved in the SWC file format, which is a widely used ASCII format for specifying neuronal morphology (e.g., used by neuromorpho.org (Ascoli *et al.*, 2007)). Multiple morphological features were selected for analysis based on these reconstructions. Extracted features provide data input for the generation of a morphology-based taxonomy, and will be integrated with taxa from other neuron attributes such as electrophysiology or transcriptomics.

Extracted features included twenty-one global morphology metrics. A subset of morphology features defined in L-Measure (<http://cng.gmu.edu:8080/Lm/help/index.htm>) (Scorcioni *et al.*, 2008) were produced in the informatics pipeline by the Vaa3D plugin “Compute Global Features” (**Table 6**). To see descriptive images of the Morphology Features (except number of nodes) for dendrites only, hover over the name to follow the hyperlink embedded in the text.

Table 6. Global morphology features and their definitions.

Morphological Feature	Definition
Number of nodes	The total number of nodes in the given input neuron (one SWC file). A node in a SWC file represents a single sample point of the neuron defined by its X, Y and Z coordinates, a radius, and its connectivity to other nodes in the neuron.
Soma surface area	The surface of the soma is computed by one of two methods. If the soma is composed of just one node then the sphere assumption is used; otherwise the sum of the external cylindrical surfaces of nodes forming the soma is calculated.
Number of stems	The number of stems attached to the soma. When the type of the node is not soma, it is labeled as a stem.
Number of bifurcations	The number of bifurcations for the given input neuron. A bifurcation point has two daughters.
Number of branches	The number of branches in the given input neuron. A branch is one or more compartments that lie between two branching points or between one branching point and a termination point.
Number of tips	The number of terminal tips for the given input neuron. This function counts the number of nodes that are terminal endpoints.
Neuronal height	Height is computed on the y-coordinates and it is the difference of minimum and maximum y-values after eliminating the outer points on either end by using the 95% approximation of the y-values of the given input neuron.
Neuronal width	Width is computed on the x-coordinates and it is the difference of minimum and maximum x-values after eliminating the outer points on either end by using the 95% approximation of the x-values of the given input neuron.
Neuronal depth	Depth is measured on the y-coordinates and it is the difference of minimum and maximum y-values after eliminating the outer points on either ends by using the 95% approximation of the y-values of the given input neuron.
Average diameter (thickness)	The average diameter of all compartments of the neuron.
Total length	The total length of the neuron is computed as the sum of distances between two connected nodes for all branches of the input neuron.
Total surface area	The total surface area of the entire neuron.
Total volume	The total volume of the entire neuron.
Maximum Euclidean distance to root	The maximum Euclidean distance of all nodes. Euclidean distance is the straight line distance from the soma (root) to the node.
Maximum path distance to root	The maximum path distance of all nodes. The path distance is the sum of lengths of all connected nodes from the soma, ending with that node.
Maximum branch order	The maximum order of the branch. A branch's order is defined with respect to the soma where the soma has a branch order = 0. The first bifurcation has a branch order = 1, the second bifurcation has a branch order = 2, and so on.
Average contraction	The average ratio between Euclidean distance of a branch and its path length. Euclidean distance of a branch is the straight-line distance from the soma to the branch. Path length is the sum of the lengths between each node along the path.
Average fragmentation	The average number of compartments that constitute a branch between two bifurcation points or between a bifurcation point and a terminal tip.
Average parent-daughter ratio	The average ratio between the diameter of a daughter branch and its parent branch. One value for each daughter branch is generated at each bifurcation point.
Average local amplitude angle	The average angle between the first two compartments (in degree) at a bifurcation.
Average remote amplitude angle	The average angle between two bifurcation points or between bifurcation point and terminal point or between two terminal points.

REFERENCES

Ascoli GA, Donohue DE, Halavi M (2007) NeuroMorpho.Org: a central repository for neuronal morphologies. *Journal of Neuroscience* 27:9247-9251.

Braitenberg V and Schuz A (1998) *Cortex: Statistics and Geometry of Neuronal Connectivity*. Second Edition. Springer-Verlag Berlin Heidelberg, New York.

Bria A, Iannello G, Onofri L, Peng H (2016) TeraFly: real-time 3D visualization and annotation of terabytes of multidimensional volumetric images. *Nature Methods* 13:192-194.

Dong HW (2008) *Allen Reference Atlas: A Digital Color Brain Atlas of the C57BL/6J Male Mouse*. Hoboken, NJ: John Wiley & Sons.

Jiang X, Shen S, Cadwell CR, Berens P, Sinz F, Ecker AS, Patel S, Tolias AS (2015) Principles of connectivity among morphologically defined cell types in adult neocortex. *Science* 350: aac9462.

Paxinos G, Franklin KBJ (2001) *The Mouse Brain in Stereotaxic Coordinates*, Second Edition. Elsevier Academic Press, San Diego, CA.

Peng H, Ruan Z, Long F, Simpson JH, Myers EW (2010) V3D enables real-time 3D visualization and quantitative analysis of large-scale biological image data sets. *Nature Biotechnology* 28:348-353.

Peng H, Long F, Myers G (2011) Automatic 3D neuron tracing using all-path pruning. *Bioinformatics* 27:i239-i247.

Peng H, Bria A, Zhou Z, Iannello G, Long F (2014) Extensible visualization and analysis for multidimensional images using Vaa3D. *Nature Protocols* 9:193-208.

Peng H, Tang J, Xiao H, Bria A, Zhou J, Butler V, Zhou Z, Gonzalez-Bellido PT, Oh SW, Chen J, Mitra A, Tsien RW, Zeng H, Ascoli GA, Iannello G, Hawrylycz M, Myers E, Long F (2014) Virtual finger boosts three-dimensional imaging and microsurgery as well as terabyte volume image visualization and analysis. *Nature Communications* 5:4342.

Scorcioni R, Polavaram S, Ascoli GA (2008) L-Measure: a web-accessible tool for the analysis, comparison and search of digital reconstructions of neuronal morphologies. *Nature Protocols* 3:866-876.

Xiao H, Peng H (2013) APP2: automatic tracing of 3D neuron morphology based on hierarchical pruning of a gray-weighted image distance-tree. *Bioinformatics* 29:1448-1454.

Zhou Z, Sorensen S, Zeng H, Hawrylycz M, Peng H (2014) Adaptive Image Enhancement for Tracing 3D Morphologies of Neurons and Brain Vasculatures. *Neuroinformatics* 1-14.

Zhou Z, Sorensen S, Peng H (2015) Neuron crawler: an automatic tracing algorithm for very large neuron images. *Proceedings of IEEE 2015 International Symposium on Biomedical Imaging: From Nano to Macro*, 870-874.